

Reevaluation of the Evaporation Method for Determining Hydraulic Functions in Unsaturated Soils

Ole Wendroth,* W. Ehlers, J. W. Hopmans, H. Kage, J. Halbertsma, and J. H. M. Wösten

ABSTRACT

Understanding of soil water and solute transport processes requires knowledge of the soil hydraulic properties. A simple evaporation method for the determination of the hydraulic conductivity function and the water retention characteristic was developed and applied to a range of soils with different texture and structure. During evaporation from the top of a 6-cm-high soil core, soil water pressure head at 1.5 and 4.5 cm below the soil surface was measured with tensiometers several times. At the same time, evaporative water loss was determined by weighing the soil column. The procedure for calculation of hydraulic functions was evaluated via numerical simulations. Results from the numerical experiment confirm the underlying theory. A limitation of the evaporation method is the fact that, at water contents near saturation where hydraulic conductivity is high, hydraulic gradients cannot be determined with sufficient accuracy. Other measurement techniques are suggested that can supplement the evaporation method in the wet range.

KNOWLEDGE of soil hydraulic properties is important for description and prediction of water and solute transport processes. These properties — the hydraulic conductivity function and the water retention characteristic — are strongly influenced by soil struc-

ture and, with decreasing water content, are increasingly influenced by soil texture. They are of particular interest in the unsaturated range near water saturation, since this range is relevant to ecologically important processes such as water infiltration, drainage, and soil aeration. A technique for easy assessment of hydraulic properties is required to quantify effects of land use and soil management on soil structure-related processes.

The determination of soil hydraulic properties is time consuming, and especially hydraulic conductivity $K(h)$, where h is the soil water pressure head, or $K(\theta)$, where θ is the water content, is difficult to obtain accurately. The major difficulty arises from the fact that hydraulic functions are highly nonlinear (Feddes et al., 1988). Thus, a small change in water content may change K and h by orders of magnitude.

Various laboratory methods have been developed for estimating $K(h)$ or $K(\theta)$ under steady-state conditions (e.g., Nielsen et al., 1960; Watson, 1967; Henseler and Renger, 1969; Klute, 1972). With steady-state laboratory methods, the time required to estimate K across a wide range of h or θ is rather long and nearly prohibitive. Moreover, problems arising from membrane resistance sometimes preclude time-invariant flux and soil water pressure head distributions across the sample (Renger et al., 1973). Therefore, several less time-consuming quasi-steady-state methods have been developed. Two examples are the hot

O. Wendroth, Institut für Bodenforschung, ZALF, Wilhelm-Pieck-Str. 72, O-1278 Müncheberg, Germany; W. Ehlers and H. Kage, Institut für Pflanzenbau und Pflanzenzüchtung, Universität Göttingen, von Siebold-Str. 8, 3400 Göttingen, Germany; J.W. Hopmans, Hydrologic Science, Dep. of Land, Air and Water Resources, Univ. of California, Davis, CA 95616; and J. Halbertsma and J.H.M. Wösten, The Winand Staring Centre for Integrated Land, Soil and Water Research, P.O. Box 125, 6700 AC Wageningen, the Netherlands. Received 24 June 1992. *Corresponding author.

Published in Soil Sci. Soc. Am. J. 57:1436–1443 (1993).

Abbreviations: K , hydraulic conductivity; h , soil water pressure head; θ , volumetric soil water content, z , depth coordinate; θ_s , θ_r , saturated and residual water content (here used as fitting parameters); α , n , m , ℓ , empirical fitting parameters; q , volume flux density of water; V , water storage; S , degree of water saturation; K_s , saturated hydraulic conductivity (here used as a fitting parameter); ER, evaporation rate; ρ_b , soil bulk density; t , time.

air method (Arya et al., 1975) and the sorptivity method (Dirksen, 1979). Van Grinsven et al. (1985) reported that the hot air method is best adaptable for loamy soils. For clayey soils, however, the evaporation time is too long for an adequate $\theta(z)$ resolution, where z denotes the soil depth, while for sandy soils the energy required to obtain zero water content at the soil surface is exceptionally high. Moreover, the influence of experimental nonisothermal conditions on soil hydraulic properties is not known and therefore neglected. Use of the sorptivity method is more or less restricted to coarse-textured soils, probably because in fine-textured soils the wetting front initially advances slowly and unevenly in the sample.

In the past, several evaporation methods have been developed for soil columns with simultaneous measurement of evaporation and soil water pressure head. Different numbers of tensiometers at various heights have been examined (Wind, 1968; Flocker et al., 1968; Becher, 1971; Schindler, 1980; Kraemer, 1987; Plagge et al., 1990). Nonlinearity of water content and soil water pressure head profiles during evaporation caused several investigators to use many tensiometers along the direction of flow. However, Schindler (1980) measured soil water pressure head at only two depths and reported promising results for soils with a wide range of textures (Schindler et al., 1985).

The objective of this study was to estimate both the hydraulic conductivity function and the water retention characteristic experimentally from soil water pressure head measurements at only two depths and from evaporative total water loss, determined simultaneously. The simple setup, similar to the one reported by Schindler (1980), was combined with a calculation procedure proposed by Wind (1968). For the estimation of water fluxes, a quasistationary approach was used. A second aim was to examine the precision of this quasistationary approach. Therefore, the hydraulic functions of three differently textured soils, measured with the evaporation method, were used as inputs in a numerical simulation, accounting for nonlinearity of hydraulic properties by a high resolution of soil depth. The boundary conditions were set and the simulated results were handled as in the evaporation experiments. The quasistationary calculation procedure was applied to simulated soil water pressure head and evaporative water loss data. The results obtained were compared with the hydraulic functions given as model input, in order to examine the assumptions underlying the quasistationary approach.

MATERIALS AND METHODS

The evaporation method was applied to three differently textured soils (Table 1), a sandy loam (Ap horizon from an Udipsamment, located in Bruchköbel), a silty loam (A2 horizon from a Typic Hapludalf, located in Hottenrode) and a clay (B horizon from a Typic Eutrochrept, located in Waake). The difference in the silt-sand threshold particle diameter between U.S. (0.05 mm) and German (0.063 mm) classification systems was neglected for classifying the soils in this study.

An undisturbed soil core sample with a height of 6 cm and inside diameter of 8 cm was placed on a ceramic plate and saturated with deionized water. Two tensiometers (ceramic material P80, Staatliche Porzellanmanufaktur, Berlin, Ger-

Table 1. Sampling location, horizon, depth, texture, and bulk density (ρ_b) for the three different German soils in this study.

Location	Horizon	Depth cm	Textural class	Sand Silt Clay			ρ_b Mg m ⁻³
				— g kg ⁻¹ —			
Bruchköbel	Ap	10–16	Sandy loam	580	360	60	1.70
Hittenrode	A2	80–86	Silty loam	40	800	160	1.42
Waake	B	40–46	Clay	20	400	580	1.41

many)¹ with cups of 6-cm length and 0.6-cm o.d. were then horizontally inserted into drill holes in the soil core at 1.5 and 4.5 cm from the sample surface (Fig. 1). The ceramic cups were connected to pressure transducers (Type 136, PC 15 G3 L, Honeywell GmbH, Offenbach, Germany) with a sensitivity of 0.01 mV, equivalent to 0.25 cm of pressure.

After saturation, a hanging water column created a negative pressure equal to an initial soil water pressure head of -25 cm for the sandy loam -10 cm for the silty loam and the clay, at the reference level of 3-cm depth. Before starting evaporation, the lid-covered sample was removed from the ceramic and placed for half a day on an aluminum plate. Readings of the two tensiometers were then compared. Since hydraulic equilibrium was assumed at that time, any deviation from the 3-cm pressure difference between the tensiometers was corrected by shifting the linear calibration curve of both tensiometers. Each calibration curve was shifted by the same amount, but in opposite directions, so that exactly a 3-cm pressure difference was measured at the time evaporation was initiated.

Evaporation was then started and, after each pressure reading, transducer wires were disconnected and the soil sample with the tensiometers was weighed on a balance with 0.01-g accuracy in order to determine the evaporative water loss in time. The length of time between measurements depended on evaporation rate. At evaporation rates of about 1.5 cm d⁻¹, a

¹ Company names are included for information only, and do not imply endorsement or preferential treatment by the authors or by any research institution involved in this study.

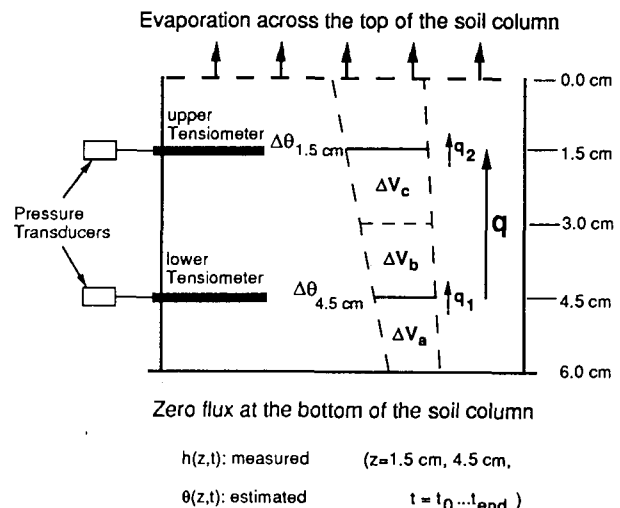


Fig. 1. Experimental setup for the evaporation method (h denotes the soil water pressure head, q the average upward volume flux density of water in the soil compartment between 1.5- and 4.5-cm depth, q_1 and q_2 the upward volume flux density of water across the 4.5- and the 1.5-cm boundaries, respectively, t the time coordinate, z the depth coordinate, ΔV_x the water storage change with respect to time in the depth compartment x , and $\Delta \theta_z$ the soil water content change with respect to time at depth z).

measurement interval of 15 to 30 min was used, while for smaller evaporation rates of 0.10 to 0.15 cm d⁻¹ the measurement interval was increased to 2 to 4 h. Under the climatic conditions in our laboratory, evaporation rates were ≈0.15 cm d⁻¹. In silty and sandy soils at high water contents, such a small evaporation rate was too low to cause measurable hydraulic gradients between tensiometers. Therefore, in the wet range of these soils, the evaporation rate was increased to approximately 1.5 cm d⁻¹ by use of a fan, blowing air away from the soil surface at room temperature. Once the gradient between tensiometers was in the range of 1.5 to 2.5 m m⁻¹, the top of the soil sample was covered again to prevent further evaporation. After a new hydraulic equilibrium was obtained, evaporation was allowed to continue without the blowing fan at a rate of approximately 0.15 cm d⁻¹. For the clay, the evaporation rate was artificially kept low at around 0.10 cm d⁻¹ by placing a perforated metal cover on top of the sample. The cover reduced drying of the soil surface with concomitant abrupt changes in soil water pressure head and conductivity at the soil surface. Generally, the evaporation experiment was terminated after the upper tensiometer recorded soil water pressure head value below -650 cm. The tensiometers were removed and total residual water content was determined by sample drying at 105 °C. For further details, see Wendroth (1990).

THEORY

Determination of Soil Hydraulic Functions

The following calculations were performed with the experimental data (see Wind, 1968). The 6-cm-high soil sample was divided into an upper (0–3-cm depth) and a lower compartment (3–6-cm depth). Water stored in both 3-cm compartments was assumed to change in time according to the soil water pressure head changes measured at the two tensiometer locations during the evaporation experiment. While assuming an initial guess for the water retention curve, tensiometric readings were converted into water contents for each of the two compartments. Unlike Wendroth (1990), who described the water retention curve with a fitted polynomial, the analytical form of $\theta(h)$

$$\theta = \theta_r + \frac{\theta_s - \theta_r}{(1 + |\alpha h|^n)^m} \quad [1]$$

was used in this study. In Eq. [1], θ_s and θ_r denote saturated and residual water content, and α , n , and m ($m = 1 - 1/n$) were used as empirical fitting parameters (van Genuchten, 1980). The water content values obtained from the initial guess of the retention curve parameters were used to determine water storage in the upper and lower compartments. Total predicted water storage was compared with the measured water storage in the soil column, obtained from weighing the soil sample at particular times. The difference between measured and predicted water storage was equally redistributed to both compartments of the soil column and water contents were then corrected. From these θ - h pairs, a new retention curve was obtained, and van Genuchten (1980) parameters were fitted to this curve using a nonlinear least-squares optimization program (RETC, M.Th. van Genuchten, 1986, unpublished data). This procedure was repeated until the changes of estimated water content values between iterations were <0.0001 m³/m³ (Column 6 in Table 2).

The average upward water flux density q in the compartment between the two tensiometers installed in the core as mentioned above (Fig. 1) can be estimated from water content changes in time by the following equation:

$$q = \frac{\int_{6.0\text{cm}}^{4.5\text{cm}} d\theta dz - \int_{6.0\text{cm}}^{1.5\text{cm}} d\theta dz}{2\Delta t} \quad [2]$$

Table 2. Update of empirical parameters† (Eq. [1]) during iterative estimation (Wind, 1968) of water retention curves for the three soils.

Number of iteration (k)	θ_s	θ_r	α	n	maximum
	m ³ m ⁻³		cm ⁻¹		($\theta_k - \theta_{k-1}$)
					m ³ m ⁻³
Sandy loam					
0	0.450	0.050	0.0400	1.200	—
1	0.321	0.134	0.0174	1.865	0.11484
2	0.321	0.135	0.0174	1.865	0.00010
3	0.321	0.135	0.0174	1.865	0.00000
Silty loam					
0	0.450	0.050	0.0400	1.200	—
1	0.522	0.000	0.1795	1.088	0.08521
2	0.523	0.000	0.1904	1.087	0.00037
3	0.524	0.000	0.1912	1.087	0.00004
Clay					
0	0.450	0.050	0.0400	1.200	—
1	0.458	0.000	0.0037	1.257	0.10172
2	0.454	0.000	0.0034	1.216	0.01680
3	0.455	0.000	0.0061	1.131	0.01375
8	0.468	0.000	0.1058	1.041	0.00136
12	0.471	0.000	0.1471	1.039	0.00001

† θ_s and θ_r are the saturated and residual water contents (used here as fitting parameters); α and n are empirical fitting parameters.

The first term in the numerator of Eq. [2] denotes volume of water flowing per unit area out of the 4.5- to 6.0-cm depth compartment into the 1.5- to 4.5-cm depth compartment, and the second term is the volume of water flowing per unit area out of that compartment (1.5–4.5-cm depth) into the 0.0- to 1.5-cm depth compartment (Fig. 1). For our experimental setup, Eq. [2] was approximated by the following quasistationary approach. Water content changes in time were assumed to increase linearly from the bottom to the top of the soil column. The average volume flux density of water in the compartment between the tensiometers (Fig. 1) was approximated by

$$q = \frac{q_1 + q_2}{2} \quad [3]$$

where q_1 is equal to the change in water storage (ΔV_a) per unit area and time in the soil compartment between 4.5 and 6.0 cm, and q_2 denotes the change in water storage ($\Delta V_a + \Delta V_b + \Delta V_c$) per unit area and time between 1.5- and 6.0-cm soil depth. The average change of water storage ΔV_x in a compartment x with thickness Δz (in this case, 1.5 cm) was computed from the water content change $\Delta\theta_x$ at the average depth in that compartment by

$$\Delta V_x = \Delta\theta_x \Delta z. \quad [4]$$

Knowing $\Delta\theta_{1.5}$ and $\Delta\theta_{4.5}$ from the estimated water retention curve, $\Delta\theta_x$ values were linearly interpolated for calculating ΔV_b and ΔV_c and extrapolated for calculating ΔV_a (Fig. 1). Hence,

$$q = \frac{\Delta V_a + (\Delta V_a + \Delta V_b + \Delta V_c)}{2 \Delta t} \quad [5a]$$

or

$$q = \frac{(3.5 \Delta\theta_{4.5} + 0.5 \Delta\theta_{1.5}) \Delta z}{2 \Delta t} \quad [5b]$$

In Eq. [5b], Δz was equal to 1.5 cm. If, in the case of the sandy loam and the silty loam, slow evaporation had been

continued immediately after fast evaporation without intermediate hydraulic equilibrium, Eq. [5] would not have been valid.

The hydraulic gradient was arithmetically averaged for each particular time interval. Once q and the gradient were determined, the hydraulic conductivity was calculated according to

$$K = - \frac{q}{\frac{dh}{dz} \Big|_{1.5} + 1} \quad [6]$$

Corresponding h and θ values for the $K(h)$ and the $h(\theta)$ relationships were calculated from

$$\bar{h} = \frac{h_{i,-1.5cm} + h_{i+1,-1.5cm} + h_{i,-4.5cm} + h_{i+1,-4.5cm}}{4} \quad [7a]$$

and

$$\bar{\theta} = \frac{\theta_{i,-1.5cm} + \theta_{i+1,-1.5cm} + \theta_{i,-4.5cm} + \theta_{i+1,-4.5cm}}{4} \quad [7b]$$

where $h_{i,z}$ and $\theta_{i,z}$ denote the measured soil water pressure head and the water content according to the estimated water retention curve, respectively, at time i and depth z . In the following, \bar{h} and $\bar{\theta}$ are denoted without the bar for $K(h)$ and $h(\theta)$.

Evaporation Simulation

In the preceding description of calculations, we assumed that the average soil water flux can be approximated by Eq. [5] from estimated water contents at two positions and the average hydraulic gradient from soil water pressure heads measured at two depths (Fig. 1). The validity of these assumptions can be examined by numerical simulations with high space and time resolutions. These simulations are not restricted to linearly increasing water content changes and the simplified hydraulic gradient calculation in the center 3-cm compartment.

Analytical functions were fitted to hydraulic properties obtained with the evaporation experiments and were used as model input. The assumption invoked by Eq. [5], [6], and [7] were evaluated by comparing the soil hydraulic properties calculated from simulated h values at 1.5- and 4.5-cm depths and afterwards iteratively estimated retention curves (Wind, 1968) with those hydraulic functions used as model input. Therefore, a fully implicit one-dimensional water flow model (J.W. Hopmans, 1988, unpublished data) was used.

The Richards equation,

$$C(h) \frac{\partial h}{\partial t} = \frac{\partial}{\partial z} \left[K(h) \frac{\partial h}{\partial z} \right] + \frac{\partial K}{\partial h} \frac{\partial h}{\partial z} \quad [8]$$

with C denoting the specific water capacity, was solved by a finite difference approximation in order to obtain h for each point in the time and space domain. Convergence of the solution for h was controlled by Picard iteration for any time step. The time step size was controlled by the mass balance.

Boundary conditions in the numerical simulations were set similar to the evaporation experiments, i.e., the upper boundary condition was the average measured evaporation rate and the lower boundary condition was equal to a zero flux. The numerical simulation was initiated at hydraulic equilibrium with $h = -10$ cm at the center of the soil sample (3-cm depth). Soil hydraulic functions were given as model input with Eq. [1] for the retention curve and

$$K(S) = K_s S^e [1 - (1 - S^{1/m})^m]^2 \quad [9]$$

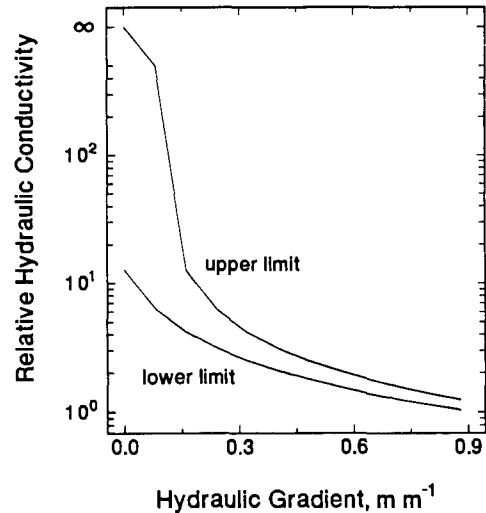


Fig. 2. Relative hydraulic conductivity, K , with respect to the water flux density, q , as a function of the hydraulic gradient.

for the hydraulic conductivity function (van Genuchten, 1980), with $S = (\theta - \theta_r)/(\theta_s - \theta_r)$, and the saturated hydraulic conductivity K_s , m ($m = 1 - 1/n$), and e as empirical fitting parameters.

RESULTS

Measurements

Pressure transducer tensiometers used for measurements had a sensitivity of ≈ 0.25 cm. Assuming that the calibration curve of the two tensiometers at 1.5- and 4.5-cm depth had the same slope, the vertical hydraulic gradient between the tensiometers could be determined only with a sensitivity of ± 0.08 $m m^{-1}$. Especially at low hydraulic gradients, this led to an uncertainty in the determination of K , shown in Fig. 2 as the range of calculated relative hydraulic conductivity with respect to the volume flux density of water. In order to obtain the upper and lower limit of calculated hydraulic conductivity at a particular gradient, relative conductivity has to be multiplied by the average flow rate q . For example, if the gradient is calculated as 0.2 $m m^{-1}$, i.e., upper and lower limits of relative conductivity are 9 and 4, respectively (Fig. 2), and the average flow rate is 0.7 $cm d^{-1}$, the hydraulic conductivity ranges from 6.3 to 2.8 $cm d^{-1}$. Notice, that this uncertainty is regardless of soil type and that the calculation of the range was based on the instrumental sensitivity only. Temporal shifts of the transducer calibration curves were neglected in this case since the recalibration after 1 d showed a shift of the calibration curve close to zero and showed an average shift of only 1 cm (min. 0.2 cm, max. 4.2 cm) after 1 yr. In view of the high uncertainty at low gradients due to the limited instrumental sensitivity, all K values obtained in the evaporation experiment from gradients < 0.2 $m m^{-1}$ were rejected in this study.

The updating of water retention curves with their parameters in Eq. [1] by the iterative estimation (Wind, 1968) is presented in Fig. 3a, 3b, and 3c and in Table 2 for all three soil types. For the sandy loam and the silty loam, convergence was reached after three iterations. The water retention curves obtained after the first iteration were close to the curves of the last iteration. For the clay, 12 iterations were necessary to reach con-

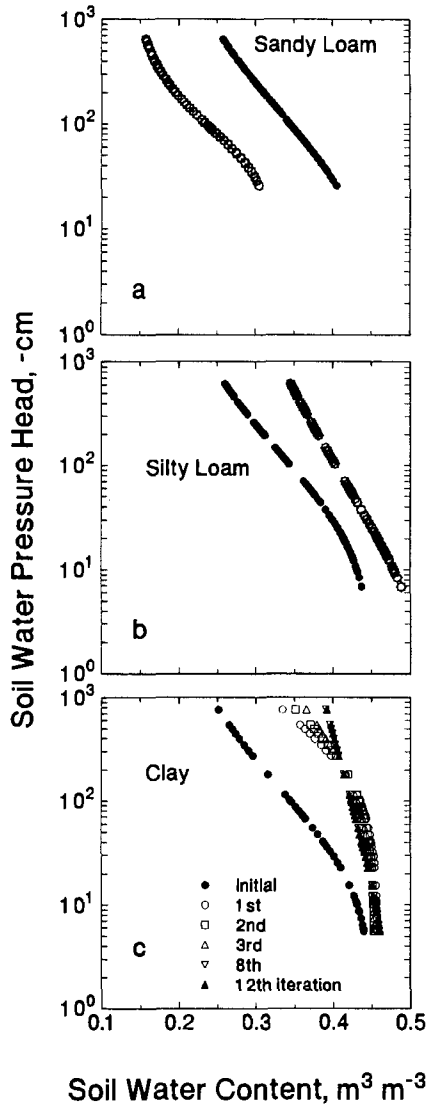


Fig. 3. Iterative estimation of water retention curves for the (a) sandy loam, (b) silty loam, and (c) clay. Estimated parameters (according to Eq. [1]) for each iteration are presented in Table 2.

vergence. This relatively high number of iterations might be reduced if the initial estimate of the retention curve was closer to that of a clayey soil.

Figure 4 shows the $h(\theta)$ and $K(h)$ relations for the three different soils, using Eq. [5], [6], and [7]. Due to the limitations of the hydraulic gradient measurements, $K(h)$ values were not calculated for the sandy loam sample at $h > -30$ cm. For the silty loam and the clay samples, K could be determined for h values smaller than -10 cm.

Model Calculations

In order to evaluate the theory behind Eq. [5], [6], and [7], $K(h)$ and $h(\theta)$ relationships obtained for the three soils were used as inputs in the numerical simulations. Therefore, parameters for the retention curve obtained from the last Wind iteration were fixed and K_s and ℓ were fitted to $K(h)$ data according to Eq. [11] (parame-

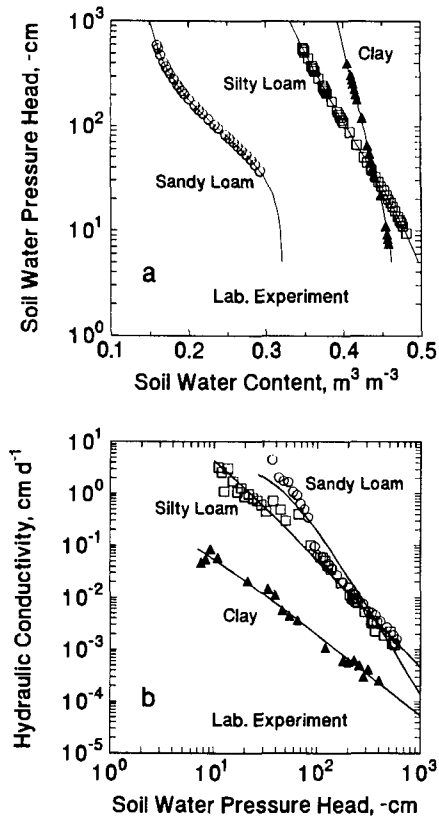


Fig. 4. (a) Water retention curves and (b) hydraulic conductivity functions for the sandy loam, silty loam, and clay, determined with the evaporation method (symbols). Curves were fitted according to Eq. [1] and [9].

ters shown in Table 3). The fitted curves are shown in Fig. 4 compared with the measured data.

Simulated soil water content and soil water pressure head profiles are shown in Fig. 5 for the three different soils with variable top boundary conditions at predefined times. Evaporation rates were similar to those measured experimentally. For the sandy loam (Fig. 5a), the evaporation rate was set at 1.56 cm d^{-1} for the first 6 h. A zero surface flux for a period of 18 h allowed equilibration, after which simulated evaporation was continued at a rate of 0.12 cm d^{-1} from that time on to 134 h. With increasing simulation time, water content profiles became slightly, and soil water pressure head profiles increasingly, nonlinear. After 134 h, the simulated cumulative amount of water evaporated from the sample surface was 0.9389 cm, while the simulated cumulative water storage change was 0.9401 cm. This mass balance

Table 3. Parameter† sets for analytical description of hydraulic soil properties (Eq. [1] and [9]) for the three soils in this study.

Soil	θ_s — $\text{m}^3 \text{ m}^{-3}$ —	θ_r	K_s cm d^{-1}	α cm^{-1}	n	ℓ
Sandy loam	0.3213	0.1346	8.43	0.0174	1.8646	-0.4509
Silty loam	0.5235	0.0000	3977.5	0.1912	1.0871	-1.1306
Clay	0.4709	0.0000	148.1	0.1471	1.0363	-12.464

† θ_s , θ_r , and K_s are saturated and residual water contents and saturated hydraulic conductivity, respectively (here used as fitting parameters; α , n and ℓ are empirical fitting parameters).

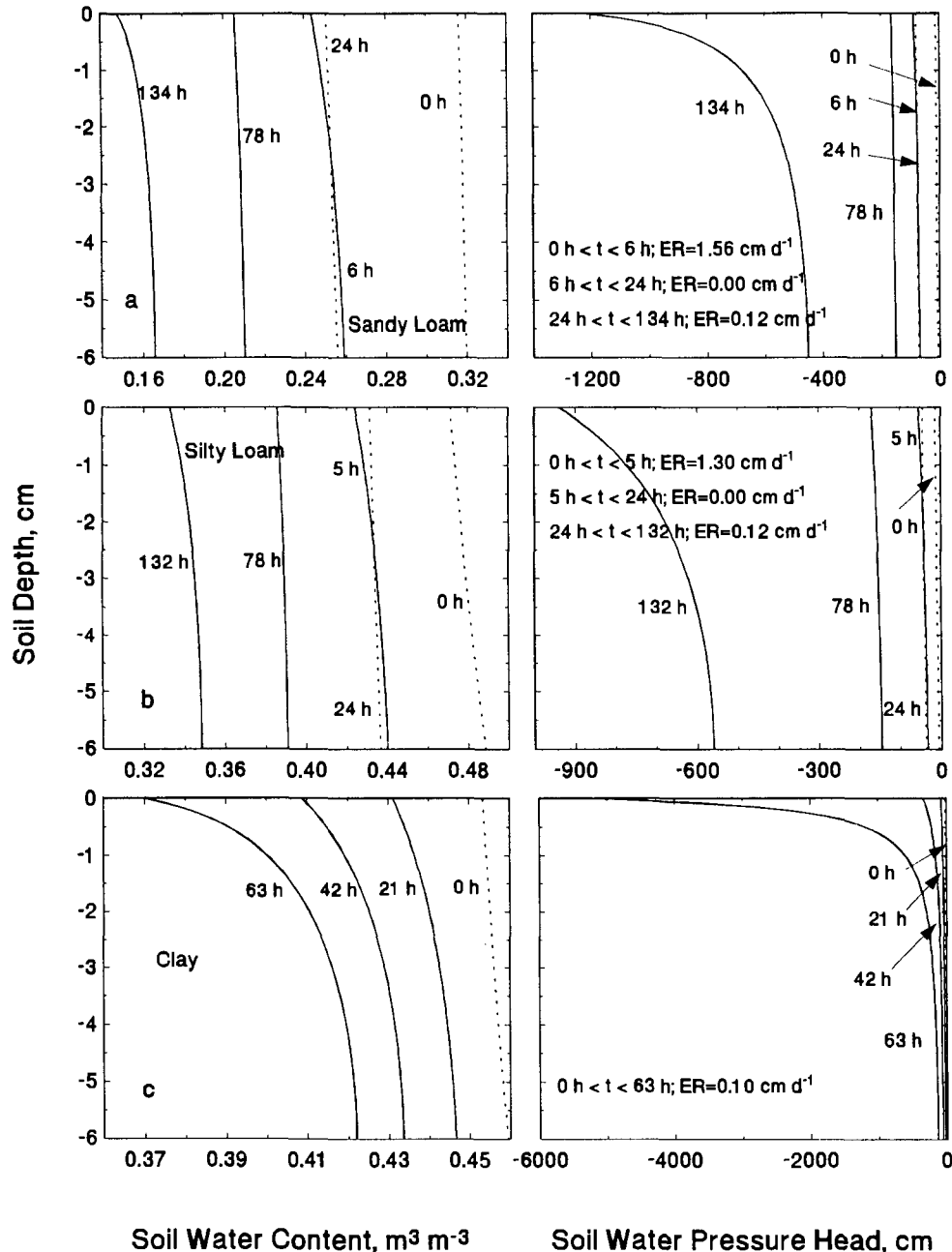


Fig. 5. Soil water content and pressure head profiles obtained from numerical simulation of evaporation for the (a) sandy loam, (b) silty loam, and (c) clay, setting various evaporation rates (ER) as the upper boundary condition.

result indicates good accuracy of the numerical model. For the silty loam (Fig. 5b), simulated evaporation rate was set high (1.30 cm d^{-1}) for the initial 5 h. After a zero surface flux between 5 and 24 h (equilibration time), simulated evaporation was continued at a rate of 0.12 cm d^{-1} . The simulated evaporation loss of water from the upper boundary and the water loss calculated from storage changes were 0.8108 and 0.8141 cm, respectively, indicating again a high model accuracy. For the clay (Fig. 5c), the evaporation rate was kept low (0.10 cm d^{-1}) continuously during the whole simulation run, as in the experiment. As expected for this soil with a steep water retention curve and a low hydraulic conductivity, the soil water pressure head profile at the end of

simulation (63 h) was highly nonlinear. Total water loss obtained from the upper boundary condition by simulation and from cumulative water storage changes was 0.2625 and 0.2686 cm, respectively, indicating a good model accuracy.

Simulated water loss and simulated soil water pressure head values at 1.5- and 4.5-cm depth only were selected for time intervals of 0.5 h during fast evaporation (sandy loam and silty loam) and for 3-h time intervals during slow evaporation (sandy loam, silty loam, and clay). Subsequently, retention curves were iteratively estimated and $K(h)$ and $h(\theta)$ were determined using Eq. [5], [6], and [7]. Hence, model results were handled as the experimental data. The results for $h(\theta)$ and $K(h)$ are shown

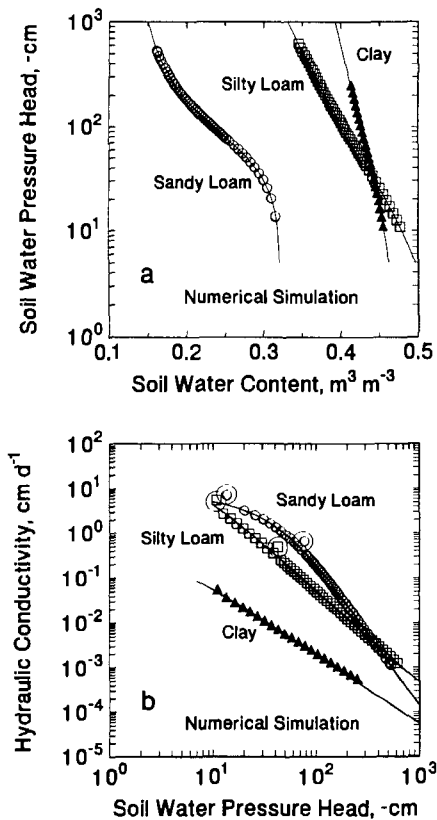


Fig. 6. (a) Water retention curves and (b) hydraulic conductivity functions for the sandy loam, silty loam, and clay. Results from evaporation simulation were applied to Eq. [5], [6], and [7] and these calculation data (symbols) were compared with model input (lines).

as symbols in Fig. 6. The comparison between these results with the curves fitted to the experimental data (lines, same as in Fig. 4), used as model input, should justify the assumptions invoked by Eq. [5], [6], and [7].

For all three soils, the results for water retention curves obtained from the simulated evaporation agreed well with retention curves used as model input (Fig. 6a). Good agreement between $K(h)$ results from the simulated evaporation and the conductivity functions given to the model was apparent as well (Fig. 6b). The average squared deviations of $\log(K)$ values between calculation and model input were 0.0022, 0.0018, and 0.0021 for the sandy loam, silty loam, and clay, respectively. For comparison, average deviations between experimental and fitted K values (Fig. 4) for the three soils were 0.0579, 0.0248, and 0.0114, respectively. Those K values (circled in Fig. 6b) calculated for time intervals immediately after the initial outset of simulated evaporation and after intermediate hydraulic equilibration were higher than expected for sandy loam and silty loam.

DISCUSSION

Validity of the Darcy equation is the major assumption in analyzing the results from both the measurements and the numerical simulation. In addition to a Darcian type of water flow, Richards equation also requires the existence of a continuous air phase in the soil column. A discontinuous air phase in the soil column, which might

have existed at moisture contents near saturation, would have reduced an increase in the hydraulic gradient between the tensiometers during evaporation. Since, in the high soil water pressure head range, the uncertainty in the determination of the hydraulic gradients was relatively high, we cannot conclude whether the measured near-zero gradients were caused by a discontinuous air phase or by high conductivities. The K values presented in Fig. 4 were calculated from apparently increasing gradients, indicating a continuous air phase. Moreover, the presented results are based on the assumption that hydraulic soil properties are the same everywhere in the soil core and do not vary with spatial scales. Using the soil hydraulic properties determined with the evaporation method for further studies, one should take into account the sample volume and scale they were measured for. We think our sample volume is a reasonable compromise for answering some of the ecologically relevant questions mentioned above.

Due to nonlinearity of soil hydraulic properties, there is no general analytical solution for the water flow equation that we could use for justifying the assumptions invoked by Eq. [5], [6], and [7]. Hence, the yard stick for validating simulated results before these results are used to evaluate our quasistationary approach is the mass balance in the numerical simulation, which showed a good accuracy of the model.

At the first time interval immediately after the outset of simulated evaporation and at the first time interval after hydraulic equilibrium, the estimated K values (quasistationary approach) for the sandy loam and the silty loam were larger than those from the hydraulic functions given as input to the model (Fig. 6b). Mass balance errors during the first time step after an abrupt change of the upper boundary condition might have caused these outliers. On the other hand, during the first time interval after the outset of evaporation, the assumption of a profile with linearly increasing water content changes with decreasing depth might not have been as valid for all subsequent time intervals. The hydraulic gradient might also have been slightly underestimated for that particular time interval, using soil water pressure head values at 1.5- and 4.5-cm depth, averaged in time. The outlier K values were calculated from gradients below 0.2 m/m, and would not have been considered for experimental results. The average hydraulic gradient in the first time interval simulated for the clay was 0.48 m m^{-1} , not causing an unexpectedly high K value. This gradient was already high enough to be considered as the mean gradient causing water flow q . Nevertheless, the overall good agreement for all three soils between model input and results obtained from our theory (Eq. [5], [6], and [7]) justifies the assumptions underlying these equations.

Most likely, the quasistationary approach leading to Eq. [5] gave good results with our experimental boundary conditions because of the relatively uniform drying of soil, i.e., flat moisture content profiles (Covey, 1963) and therefore linearly increasing water fluxes with decreasing depth over small time intervals. Covey (1963) mentioned a uniform drying of soil as long as the evaporation rate was constant and determined by external conditions only. Nevertheless, he stated that the shape of water content profiles during evaporation highly depends on sample height, soil hydraulic properties, evap-

oration rate, and initial soil water content profile. Hence, the approach postulated here, leading us to reasonable results, may not necessarily hold for different experimental designs, e.g., for other soil column lengths and other tensiometer positions and distances. Becher (1975) concluded from his evaporation experiments that three tensiometers were necessary to determine $K(h)$ in a 5-cm-high soil sample. Perhaps more tensiometers than in our experiment were needed because upper and lower tensiometers and gypsum blocks were inserted close to the boundaries of the soil column (0.5- and 4.5-cm depths). Moreover, Becher (1975) used his setup for measurements of soil water pressure heads beyond those used in our experiment, thereby causing a high nonlinearity of the h and θ profiles. The assumptions of quasistationarity might not hold in that case with measurements at two vertical positions only.

CONCLUSION

We conclude from our results that, for the range of soil textures and structures investigated, the evaporation method and the underlying calculation procedure is an elegant, simple, and inexpensive technique for determination of soil hydraulic properties. Further experiments should examine the suitability of the evaporation method for soils with extreme textures (even higher sand or clay content). A major limitation of the method is caused by the estimation of near-zero hydraulic gradients close to soil water saturation. Further experiments should show whether using different pressure transducers would allow a better resolution of small hydraulic gradients. Alternatively, the near-saturated hydraulic conductivity could be determined by steady-state infiltration methods, such as those suggested by Boels et al. (1978) or Perroux and White (1988). These infiltration methods may be applied in the saturated and near-saturated water content range at different soil water pressure heads. With decreasing pressure head, these infiltration methods become increasingly inadequate because of hardly obtainable constant fluxes and unit gradients. Once the infiltration experiment in the near-saturated range is terminated, the same soil sample can subsequently be used at lower soil water pressure heads with the evaporation method. Furthermore, this study showed that experimental designs and their boundary conditions as well as simplified calculation procedures may be examined with a preceding numerical simulation.

ACKNOWLEDGMENTS

The careful assistance of Mrs. G. Rohde during the experimental work and parts of the data analysis at Institut für Pflanzenbau und Pflanzenzüchtung, Universität Göttingen, is gratefully acknowledged. The authors are indebted to Prof. Dr. Eichhorn and Dr. Tebrügge for the opportunity to take samples of the sandy loam soil from a long-term field experiment of the Institut für Landtechnik, Universität Gießen. The project was financially supported by the German Research Foundation (DFG), Bonn. O. Wendroth is thankful for the opportunity to

finish this study during his appointment at the Department of Land, Air and Water Resources, University of California, Davis.

REFERENCES

- Arya, L.M., D.A. Farrell, and G.R. Blake. 1975. A field study of soil water depletion patterns in presence of growing soybean roots: I. Determination of hydraulic properties of the soil. *Soil Sci. Soc. Am. Proc.* 39:424-430.
- Becher, H.H. 1971. Ein Verfahren zur Messung der ungesättigten Wasserleitfähigkeit. *Z. Pflanzenernähr. Bodenkd.* 128:1-12.
- Becher, H.H. 1975. Bemerkungen zur Ermittlung der ungesättigten Wasserleitfähigkeit unter nichtstationären Bedingungen. *Z. Pflanzenernähr. Bodenkd.* 132:1-12.
- Boels, D., J.B.H.M. van Gils, G.J. Veerman, and K.E. Wit. 1978. Theory and system of automatic determination of soil moisture characteristics and unsaturated hydraulic conductivities. *Soil Sci.* 126:191-199.
- Covey, W. 1963. Mathematical study of the first stage of drying of a moist soil. *Soil Sci. Soc. Am. Proc.* 27:130-134.
- Dirksen, C. 1979. Flux-controlled sorptivity measurements to determine soil hydraulic property functions. *Soil Sci. Soc. Am. J.* 43:827-834.
- Feddes, R.A., P. Kabat, P.J.T. van Bakel, J.J.B. Bronswijk, and J. Halbertsma. 1988. Modelling soil water dynamics in the unsaturated zone — state of the art. *J. Hydrol. (Amsterdam)* 100:69-111.
- Flocker, W.J., M. Yamaguchi, and D.R. Nielsen. 1968. Capillary conductivity and soil water diffusivity values from vertical soil columns. *Agron. J.* 60:605-610.
- Henseler, K.L., and M. Renger. 1969. Die Bestimmung der Wasserdurchlässigkeit im wasserungesättigten Boden mit der Doppelmembran-Druckapparatur. *Z. Pflanzenernähr. Bodenkd.* 122:220-228.
- Klute, A. 1972. The determination of the hydraulic conductivity and diffusivity of unsaturated soils. *Soil Sci.* 113:264-276.
- Krahmer, U. 1987. EDV-gestütztes Mess- und Auswerteverfahren zur Bestimmung der ungesättigten Wasserleitfähigkeit nach der Verdunstungsmethode. *Z. Pflanzenernähr. Bodenkd.* 150:392-394.
- Nielsen, D.R., D. Kirkham, and E.R. Perrier. 1960. Soil capillary conductivity: Comparison of measured and calculated values. *Soil Sci. Soc. Am. Proc.* 24:157-160.
- Perroux, K.M., and I. White. 1988. Designs for disc permeameters. *Soil Sci. Soc. Am. J.* 52:1205-1215.
- Plagge, R., M. Renger, and C.H. Roth. 1990. A new laboratory method to quickly determine the unsaturated hydraulic conductivity of undisturbed soil cores within a wide range of textures. *Z. Pflanzenernähr. Bodenkd.* 153:39-45.
- Renger, M., W. Giesel, and O. Strebel. 1973. Der Einfluss des Übergangswiderstandes bei Wasserleitfähigkeitsmessungen an ungesättigten Bodenproben mit der Doppelmembran-Druckapparatur. *Z. Pflanzenernähr. Bodenkd.* 133:99-102.
- Schindler, U. 1980. Ein Schnellverfahren zur Messung der Wasserleitfähigkeit im teilgesättigten Boden an Stechzylinderproben. *Arch. Acker- Pflanzenbau Bodenkd.* 24:1-7.
- Schindler, U., K. Bohne, and R. Sauerbrey. 1985. Comparison of different measuring and calculating methods to quantify the hydraulic conductivity of unsaturated soil. *Z. Pflanzenernähr. Bodenkd.* 148:607-617.
- van Genuchten, M.Th. 1980. A closed-form equation for predicting the hydraulic conductivity of unsaturated soils. *Soil Sci. Soc. Am. J.* 44:892-898.
- van Grinsven, J.J.M., C. Dirksen, and W. Bouten. 1985. Evaluation of the Hot Air Method for measuring soil water diffusivity. *Soil Sci. Soc. Am. J.* 49:1093-1099.
- Watson, K.K. 1967. The measurement of the hydraulic conductivity of unsaturated porous materials utilizing a zone of entrapped air. *Soil Sci. Soc. Am. Proc.* 31:716-720.
- Wendroth, O. 1990. Koeffizienten des Wasser- und Gestransportes zur Ableitung von Kenngrößen des Bodengefüges. Ph.D. diss. Inst. f. Pflanzenbau und Pflanzenzüchtung, Universität Göttingen, Germany.
- Wind, G.P. 1968. Capillary conductivity data estimated by a simple method. p. 181-191. In P.E. Rijtema and H. Wassink (ed.) *Water in the unsaturated zone. Proc. Wageningen Symp. June 1966. Vol. 1. IASAH, Gentbrugge.*